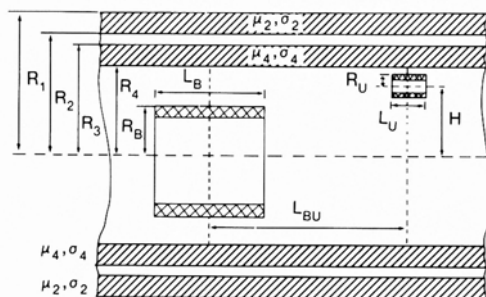


S. G. Marinov
Dresser Atlas
Houston, Texas

The presence of more than one string makes downhole inspection by electromagnetic methods more difficult not only in terms of data acquisition but also in terms of data interpretation. This occurs because the tool response is strongly influenced by the additional string, especially for the eddy current tools employed to measure wall thickness of pipes. As a result, inspection logs which are currently evaluated by experimental charts for the single string might be incorrectly interpreted with the multiple strings. In order to avoid this problem, charts should be corrected with each additional string.

The basic theory of the eddy current method has been developed in [1-2] and later amended for this application in [3].



1673

Theoretical results obtained in [1-3] have been repeatably verified experimentally so we can use the most general expressions obtained in [3] for the voltage "V_{BH}" induced into the sensor coil (Figure 1):

$$R_U + H_U < R_B$$

$$V_{BH} = A \int_0^{\infty} I_1(\lambda R_B) \times \left[\int_0^1 I_1(\lambda \sqrt{R_U^2 + H_U^2} + 2R_U H_U \cos 2\pi t) dt \right] \times F_{BH}(\lambda) \sin\left(\frac{L_B \lambda}{2}\right) \sin\left(\frac{L_U \lambda}{2}\right) \cos(L_{BU} \lambda) \frac{1}{2} d\lambda \quad (1)$$

$$R_U + H_U \geq R_B$$

$$V_{BH} = A \int_0^{\infty} I_1(\lambda R_B) \times \left[\int_0^1 I_1(\lambda \sqrt{R_U^2 + H_U^2} + 2R_U H_U \cos 2\pi t) dt \right] \times F_{BH}(\lambda) \sin\left(\frac{L_B \lambda}{2}\right) \sin\left(\frac{L_U \lambda}{2}\right) \cos(L_{BU} \lambda) \frac{1}{2} d\lambda \quad (2)$$

$$\text{where: } A = \frac{-j \omega \mu_0 R_B R_U N_B N_U}{L_B L_U}$$

and where "F_{BH}" is determined from recurrent formulas obtained in (2) for two strings.

$$F_{BH}(\lambda) = \frac{K_1(\lambda R_4) + P_4 K_0(\lambda R_4)}{I_1(\lambda R_4) - P_4 I_0(\lambda R_4)} I_1(\lambda R_B) I_1(\lambda R_U) \quad (3)$$

and where:

$$P_4 = \frac{\mu_4}{q_4} \frac{F_{11}(U_{43}, U_{44}) + \frac{q_4}{\mu_4} P_3 F_{01}(U_{43}, U_{44})}{F_{10}(U_{43}, U_{44}) + \frac{q_4}{\mu_4} P_3 F_{00}(U_{43}, U_{44})} \quad (4)$$

$$P_3 = \frac{1}{\lambda} \frac{F_{11}(U_{\lambda 2}, U_{\lambda 3}) + \lambda P_2 F_{01}(U_{\lambda 2}, U_{\lambda 3})}{F_{10}(U_{\lambda 2}, U_{\lambda 3}) + \lambda P_2 F_{00}(U_{\lambda 2}, U_{\lambda 3})} \quad (5)$$

$$P_2 = \frac{2}{q_2} \frac{F_{11}(U_{21}, U_{22}) + \frac{q_2}{\mu_2} P_1 F_{01}(U_{21}, U_{22})}{F_{10}(U_{21}, U_{22}) + \frac{q_2}{\mu_2} P_1 F_{00}(U_{21}, U_{22})} \quad (6)$$

$$P_1 = -\frac{1}{\lambda} \frac{K_1(\lambda R_1)}{K_0(\lambda R_1)} \quad (7)$$

$$\begin{aligned}
U_{43} &= q_4 R_3 \\
U_{\lambda 2} &= \lambda R_2 \\
U_{21} &= q_2 R_1 \\
U_{44} &= q_4 R_4 \\
U_{\lambda 3} &= \lambda R_3 \\
U_{22} &= q_2 R_2 \\
q_2 &= \sqrt{\lambda^2 + k_2^2}; \\
q_4 &= \sqrt{\lambda^2 + k_4^2}; \\
k_2 &= \sqrt{-j\omega \mu_2 \mu_0 \sigma_2}; \\
k_4 &= \sqrt{-j\omega \mu_4 \mu_0 \sigma_4};
\end{aligned} \tag{8}$$

where (fig. 1)

- ω is a frequency of excitation: $j = \sqrt{-1}$
- μ_4 is a magnetic permeability of inside pipe:
- μ_2 is a magnetic permeability of outside pipe:
- μ_0 is a magnetic permeability of the free space:
- σ_4 is an electrical conductivity of inside pipe:
- σ_2 is an electrical conductivity of outside pipe:
- " R_B " is an equivalent radius of the exciting coil determined according to [2]:
- " R_U " is an equivalent radius of the sensor coil also determined according to [4]:
- " L_B " is a length of exciting coil:
- " L_U " is a length of sensor coil:
- " L_{BU} " is an axial distance between the exciting coil and the sensor:
- " H_U " is a distance between axes of exciting and sensor coils:
- " N_B " is a number of turns in the exciting coil
- " N_U " is a number of turns in the sensor coil
- $j = \sqrt{-1}$

and where:

$$\begin{aligned}
 F_{11} &= K_1 \cdot I_1 - I_1 \cdot K_1 \\
 F_{01} &= K_0 \cdot I_1 + I_0 \cdot K_1 \\
 F_{10} &= K_1 \cdot I_0 + I_1 \cdot K_0 \\
 F_{00} &= K_0 \cdot I_0 - I_0 \cdot K_0
 \end{aligned}
 \tag{9}$$

I_0, K_0, I_1, K_1 are modified Bessel functions of the first and second kind, order zero and one, respectively.

Now we can examine the amplitude and the phase characteristics for the one of two strings of pipe and find conditions when their logs are clearly different from each other.

As has been pointed out in [3], a spacing between transmitter and receiver coils as well as a frequency of the excitation substantially influences both amplitude and phase, so by varying those parameters, we will try to find those conditions.

First we look at the amplitude and phase characteristics calculated from the formula (2) for the single string of pipe.

The result of calculation for two spacings and two common frequencies using formula (2) are presented on Figures 2 through 5.

(Typical parameters of pipes are used):

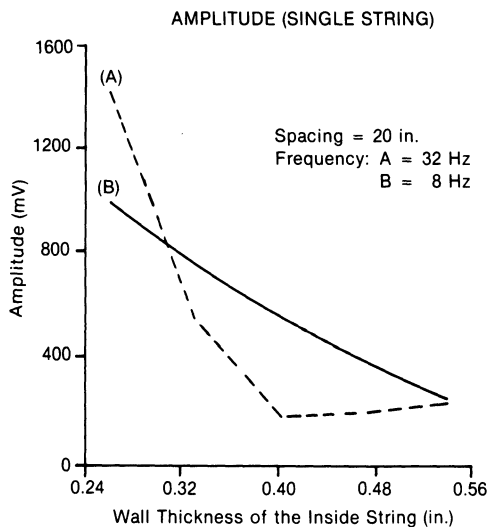


Figure 2

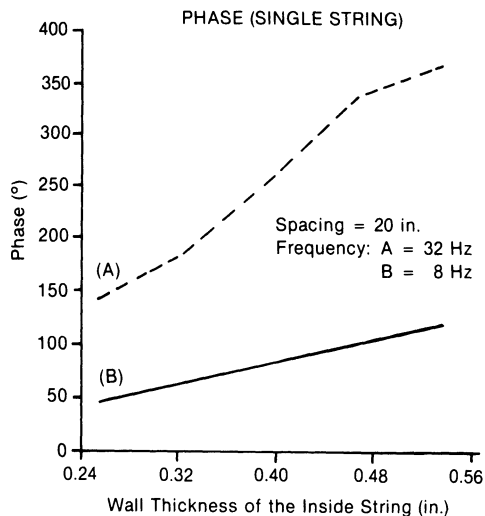


Figure 3

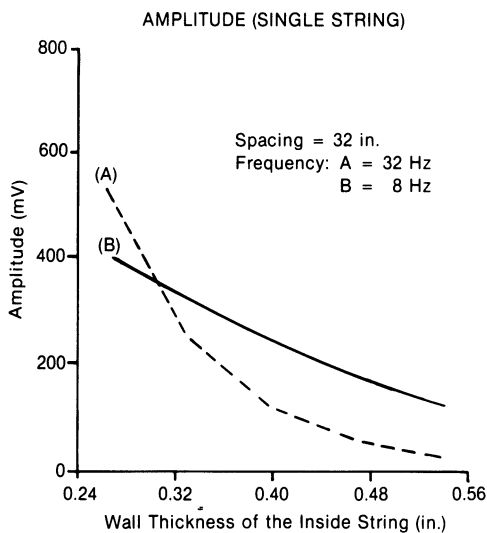


Figure 4

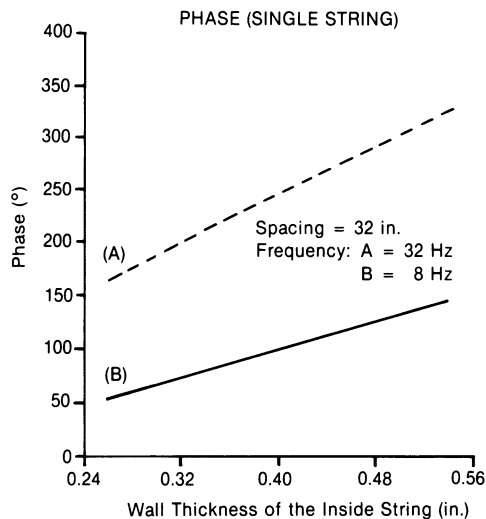


Figure 5

As we could expect, amplitudes with 20" spacing (Figures 2 and 4) are higher but the phase characteristics are not as linear as for 32" (Figures 3 and 5) especially for the frequency 8 Hz. The same things have been observed experimentally in [3] and [4].

For two strings of pipe, the log interpretation becomes considerably more complicated because in many practical cases there is a need to discriminate between changes in the wall thickness of the inside and outside strings. That is why we have to consider those cases separately.

Results of calculation of the induced voltage using formula (2) for two strings: the same 7 inch outside diameter pipe inside of 11 inch outside diameter pipe for the same 20" spacing and the same frequencies are presented on Figures 6 and 9.

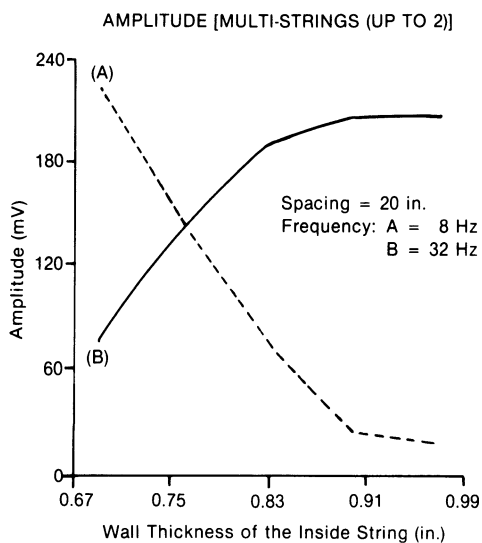


Figure 6

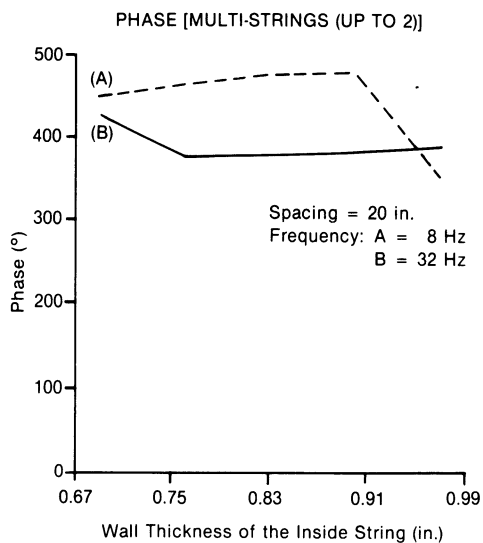


Figure 7

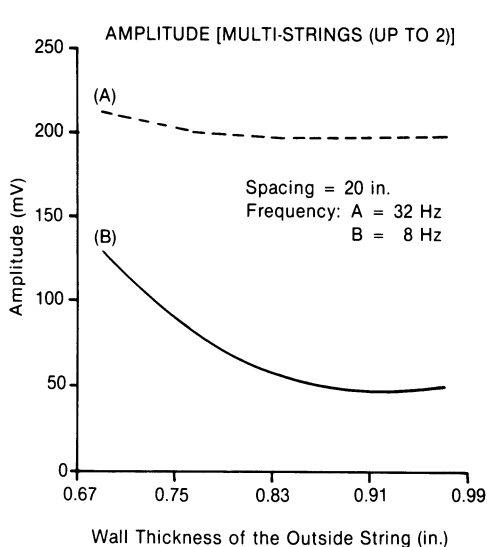


Figure 8

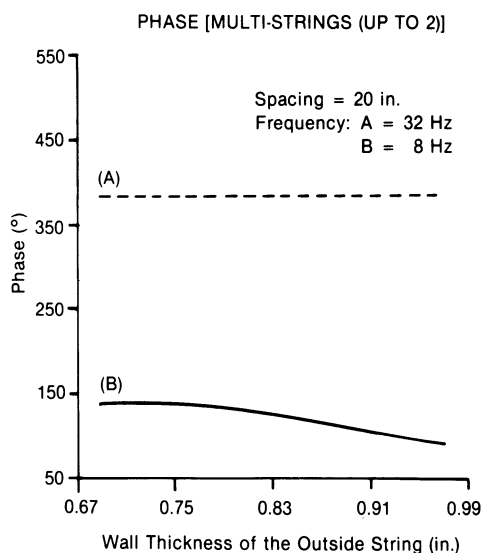


Figure 9

As we can see, both the amplitude and the phase characteristics are quite different for inside and outside strings (Figures 6 and 8, and Figures 7 and 9, respectively). That is especially true for the amplitude characteristics where even a behavior of curves is changed from inside to outside string (Figures 6 and 8). This gives an important clue to interpretation of the logs for two strings. However, this particular spacing (20") does not provide linear phase characteristics which are the major means to monitor changes in the wall thickness of either pipe. That's why we need to increase spacing to 32" although naturally the amplitude becomes smaller. The results of calculation for this spacing are presented on Figures 10 through 13.

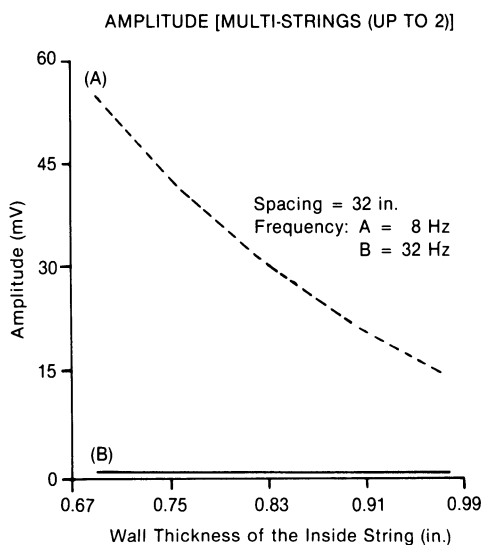


Figure 10

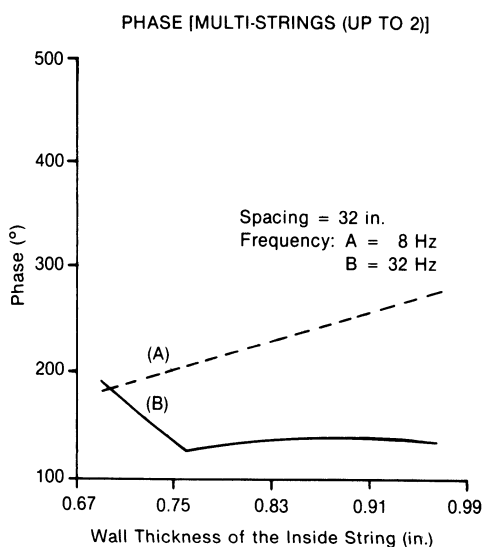


Figure 11

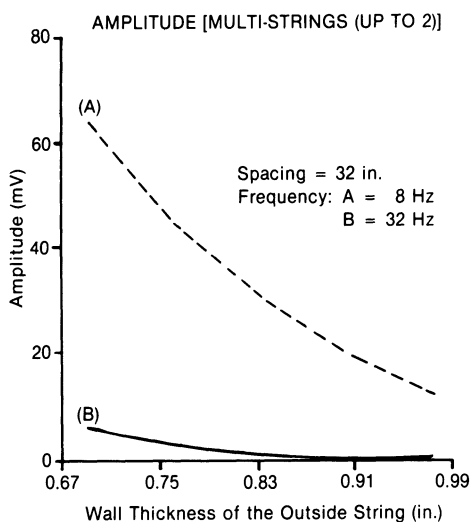


Figure 12

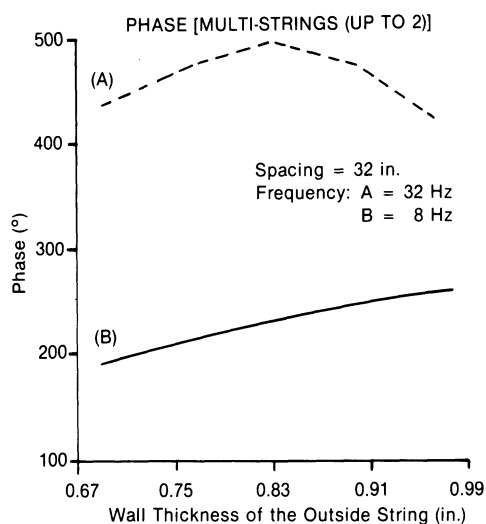


Figure 13

Here we have a somewhat different situation. While the amplitude characteristics are more similar to each other (Figures 10 and 12), the phase characteristics are clearly different (Figures 11 and 13). Also, in this case, there is a different frequency for the inside and outside string where the phase changes are linear (the curve "A" on Figure 11 and the curve "B" on Figure 13). That provides valuable information not only for the log interpretation but also for the tool's design.

The results of this investigation demonstrate that the computer models considered here provide a reliable way to improve the log interpretation for two strings of pipe and also can help in the tool's design.

1. C. V. Dodd and W. E. Deeds "Analytical Solutions to Eddy Current Probe-Coil Problems", J. Appl. Phys., 39, (1968).
2. V. C. Cerasimov "Theory of Eddy Current Transducers for Inspection of Cylindrical Specimen", Nauka, Moscow, (1972) in Russian.
3. S. C. Marinov "Theoretical and Experimental Investigation of Eddy Current Inspection of Pipes with Arbitrary Position of Sensor Coils", in 'Review of Progress in Quantitative Evaluation', edited by D. O. Thompson and D. E. Chimenti, Vol. 5A, Plenum Press, N. Y., 1986.
4. T. R. Schmidt, "The Remote Field Eddy Current Inspection Technique", Materials Evaluation, February, 1984.